

Article

Experimental Investigation of Solidification in the Cast Mold with a Consumable Cooler Introduced Inside

Ran Niu ¹, Baokuan Li ^{1,*}, Zhongqiu Liu ¹, Lifu Bu ¹, Xianglong Li ¹, Xiao Yang ² and Fumitaka Tsukihashi ²

¹ School of Metallurgy, Northeastern University, Shenyang 110819, China; niuran0331@126.com (R.N.); liuzq@smm.neu.edu.cn (Z.L.); 17074020019@163.com (L.B.); 1989lixianglong@sina.com (X.L.)

² Graduate School of Frontier Science, The University of Tokyo, Kashiwanoha 5-1-5, Kashiwa 2778561, Japan; xiao.yang@edu.k.u-tokyo.ac.jp (X.Y.); tukihasi@edu.k.u-tokyo.ac.jp (F.T.)

* Correspondence: libk@smm.neu.edu.cn; Tel.: +86-24-83672216

Received: 6 December 2018; Accepted: 7 January 2019; Published: 9 January 2019



Abstract: The microstructure is of great significance for the stability and mechanical performance of the cast slab. Recently, an innovative technology of feeding a consumable cooler into the mold has been proposed to improve the internal quality of castings. But the mechanism is not clear. In the present work, a water-cooled transparent laboratory equipment was set up and solidification of NH_4Cl -70% H_2O solution was studied to observe the in-situ growth and sedimentation of crystals. The experiments were conducted with and without adding a consumable cooler. Morphology variation of the solidification structure was visualized and temperature distribution during the process was recorded. Results show that introduction of the consumable cooler significantly reduces the temperature of the central zone. Melting of the consumable cooler can supply a large quantity of equiaxed crystals, which prevent the growth of columnar dendrites and thereby promote columnar to equiaxed transition (CET). Moreover, the enhanced convection shows an effect of grain refinement.

Keywords: NH_4Cl - H_2O solution; solidification; crystallization; dendrite growth; CET

1. Introduction

Quality and reliability of the castings are heavily dependent on the crystal structure and their homogeneity. Internal central segregation and porosity are common defects in the continuous casting (CC) slab and these defects affect the internal quality of the final rolled plate. Reducing the defects is essential for achieving satisfactory properties in the products [1]. Many methods including the low superheat pouring technique [2], the Electromagnetic Stirring (EMS) [3] and the ultrasonic vibration [4] have been implemented to reduce the defects. All these methods tend to improve the homogeneity and the amount of equiaxed crystals in the cast slab [5]. Nevertheless, the efficiency of these techniques is limited by different reasons, such as submerged entry nozzle (SEN) clogging, the size and shape of the slab [6], etc. Generally, the slab quality can be improved by generating a large amount of equiaxed grains and promoting a columnar to equiaxed transition (CET). Recently, an innovative method of feeding a consumable steel strip to the mold has been proposed by the Azovstal' Metallurgical Combine in Ukraine and the Kawasaki Steel Corporation in Japan, which can alleviate the central segregation and porosity defects of CC slab [7–10]. For the new technology, a thin consumable strip is continuously fed into the CC mold through a strip “feeder” at a desired feeding speed. The melt superheat in the central zone of the mold is decreased by the phase change decalescence of the cold strip. Melting of the cold strip can promote the formation of equiaxed grains while hindering the growth of columnar dendrites. A new pattern of solidification proceeding simultaneously at the outside and inside of

the slab eliminates the centerline segregation and improves the internal consistency. However, the mechanism underlying the improvement of internal defects by this technology is not clear because of the opaque mold as well as the harsh casting environment.

In 1965, Jackson tested several transparent compounds showing a similar pattern to metals during solidification [11]. From then on, $\text{NH}_4\text{Cl-H}_2\text{O}$ solution has been widely adopted for experimental studies of the fluid motions associated with crystallization and solidification processes. Christenson et al. [12] studied the solidification of $\text{NH}_4\text{Cl-H}_2\text{O}$ solution in a rectangular cavity with varying initial concentrations and cooling conditions. Tatsuo et al. [13] studied the detailed information of double-diffusive convection during solidification by performing the experiment of solidification of $\text{NH}_4\text{Cl-H}_2\text{O}$ solution in a rectangular chamber with lateral cooling. Beckermann and Wang [14] experimentally studied the flow field during equiaxed dendritic solidification of $\text{NH}_4\text{Cl-H}_2\text{O}$ solution. Shigeo et al. [15] used a potassium permanganate dye to trace fluid motion within the sidewall mushy region during a two sides chilling solidification. Kharicha et al. [16] used the PIV technique to study the flow pattern and the equiaxed crystal motion during an equiaxed/columnar solidification process. Zhong et al. [17] investigated the effect of crystal rain produced from the free surface on columnar to equiaxed transition. Nevertheless, investigation of the solidification process with a consumable cooler is still absent.

In the present work, solidification process of $\text{NH}_4\text{Cl-H}_2\text{O}$ solution in a cavity cooled from two sidewalls was experimentally investigated. The columnar dendrites growth from two cooling sidewalls and the equiaxed crystals motion were studied. The influences of the crystals generated from the solid consumable cooler on the solid structure and the occurrence of the CET were investigated. Related mechanisms are herein discussed.

2. Experimental Procedure

A solution of $\text{NH}_4\text{Cl-70}\%\text{H}_2\text{O}$ was used in the transparent experimental study of solidification and crystallization. The thermophysical properties of $\text{NH}_4\text{Cl-70}\%\text{H}_2\text{O}$ solution is shown in Table 1. The experiments were performed in a cavity made of acrylic with two 1-mm-thick cooper plates as two side vertical walls. Two cooling water tanks were set immediately adjacent to the two side walls. Three thermocouples with diameter 5 mm were positioned in the Y-Z median plane of the cavity at positions 2.5 mm (T3), 12.5 mm (T2) and 22.5 mm (T1) relative to the left cooling plate and were directly in contact with the $\text{NH}_4\text{Cl-H}_2\text{O}$ solution. The schematic diagram of the experiment set up is shown in Figure 1. During the solidification process, the two sidewalls of the cavity were rendered towards cooling by pumping the cold water into the tank at a given rate. The cooling water was supplied by a thermostat water bath with a mixture of ice and water. The top, front, back and bottom walls of the cavity were well insulated, leaving a slit for the light sheet and cooler adding in the top plate. A double cavity Nd-YAG laser was used as the light source. A camera monitoring system was also set up to visualize the crystallization process from the front plate. The output data of the thermocouples were displayed on a computer. The schematic diagram of the experimental system is shown in Figure 2.

Table 1. Thermophysical properties data for $\text{NH}_4\text{Cl-70}\%\text{H}_2\text{O}$ [14].

Property	Value
Density of the liquid phase, ρ_f (kg/m^3)	1078
Density of the solid ammonium chloride, ρ_s (kg/m^3)	1527.4
Dynamic viscosity of the liquid phase, μ_f (N s/m^2)	0.0013
Thermal conductivity of the liquid phase, k_f (W/m K)	0.468
Thermal conductivity of the solid phase, k_{fs} (W/m K)	2.7
Specific heat of the liquid phase, c_f (J/kg K)	3249
Specific heat of the solid phase, c_s (J/kg K)	1827
Thermal expansion coefficient, β_T ($1/\text{K}$)	3.832×10^{-4}
Latent heat of fusion at T_E , Δh (J/kg)	3.138×10^5
Eutectic temperature, T_E (K)	259.2
Liquidus temperature, T_L (K)	310.2

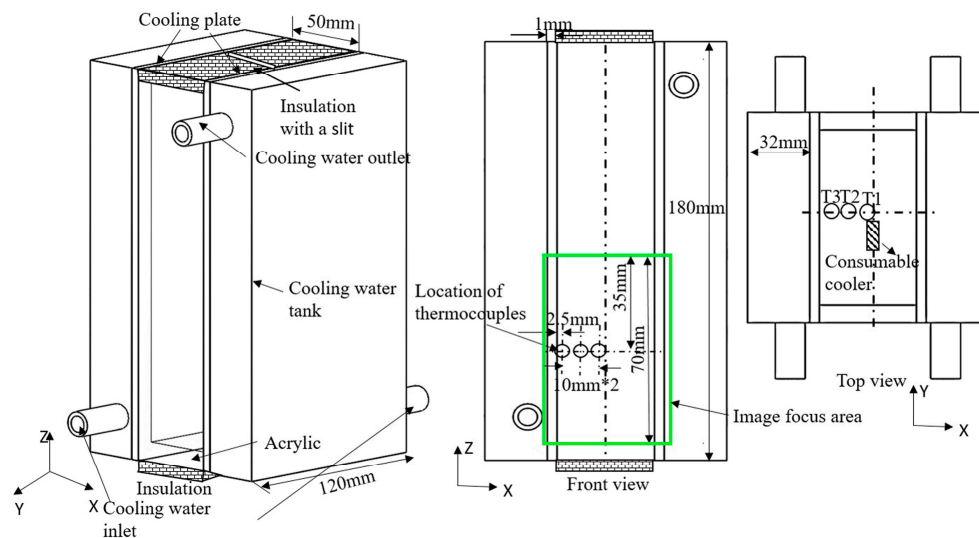


Figure 1. The schematic diagram of the experiment set up.

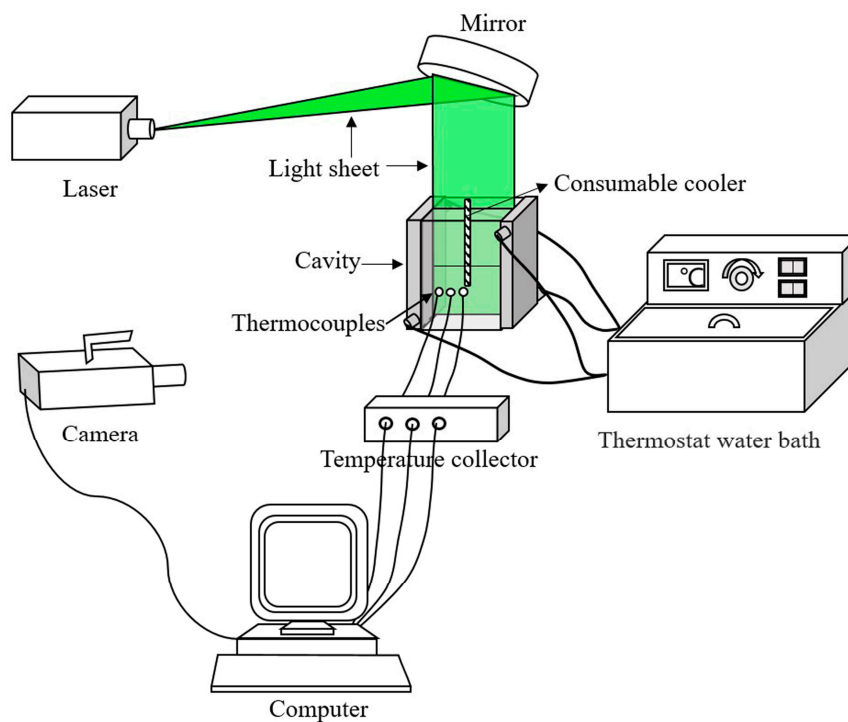


Figure 2. The schematic diagram of the experimental system.

Details about the experimental procedure are as follows. The solution of $\text{NH}_4\text{Cl-H}_2\text{O}$ was heated to $85\text{ }^\circ\text{C}$. After complete melting, the solution was poured into a cavity preheated to $85\text{ }^\circ\text{C}$ to make a 70 mm-deep bath. Later, cooling water was pumped to the tanks to trigger the solidification. At every 100 s interval, the insulation of the front plate was removed to photograph the progress of solidification. Solidification with a consumable cooler was also investigated. By the time the solidification started, a laboratory consumable cooler was immersed into the solution bath center with an immersed length of 30 mm. The consumable cooler was prepared by cooling the $\text{NH}_4\text{Cl-H}_2\text{O}$ solution in a cuboid shape mold in a freezer. Three coolers with different sizes (cross section: $3 \times 10\text{ mm}^2$, $5 \times 10\text{ mm}^2$ and $7 \times 10\text{ mm}^2$) were prepared to investigate the influence of cooling efficiency on the solidification process. The temperature measuring experiments were conducted separately from the observation experiments to ensure that there was no interference with the morphology of the solidification front.

3. Results and Discussion

3.1. Dendrite Growth during Solidification

The solidification morphology in the cavity at selected moments is shown in Figure 3. In the initial stage, after cooling for 300 s, in Figure 3a, the frozen thickness grown from the mold walls, and the bottom corner towards the inside can be seen. The frozen area was made up with columnar dendrites which were not completely perpendicular to the cooling plate but instead inclined upwardly at an angle, indicating an upward liquid flow in the columnar front in the liquid phase. With the proceeding of solidification, a few small equiaxed grains appeared (see Figure 3b). This can be understood as the NH_4Cl crystals “breaking off” at the dendritic mushy region, which had little effect on the growth of columnar dendrites. In the third stage, numerous larger equiaxed crystals presented in the lower part of the cavity, which indicated the occurrence of crystal rain (see Figure 3c). Some of these equiaxed grains were generated from the initial cooling wall and driven to the central zone by thermal convection. Others were generated from the columnar dendrite fragments [18] and transported by the fluid flow or carried down by gravity. The equiaxed crystals settled at the bottom of the cavity or were captured by the columnar dendrites in the lower part of the cavity. In the following stage of solidification, as shown in Figure 3d, the equiaxed crystals ahead of the columnar front continued to grow towards the melt. The CET occurred when the equiaxed crystals sediment bed grew to the height corresponding to the location. Solidification ended after 1400 s when the frozen area covered about 60% of the domain (including the mushy zone). The V shape’s frozen thickness consisted of both the columnar dendrites grown from the two cooling plates and the equiaxed crystals aggregated in the bottom regions. The liquid in the center region was mostly water. The schematic diagram of the development of various microscopic structural zones in a cast mold is shown in Figure 4.

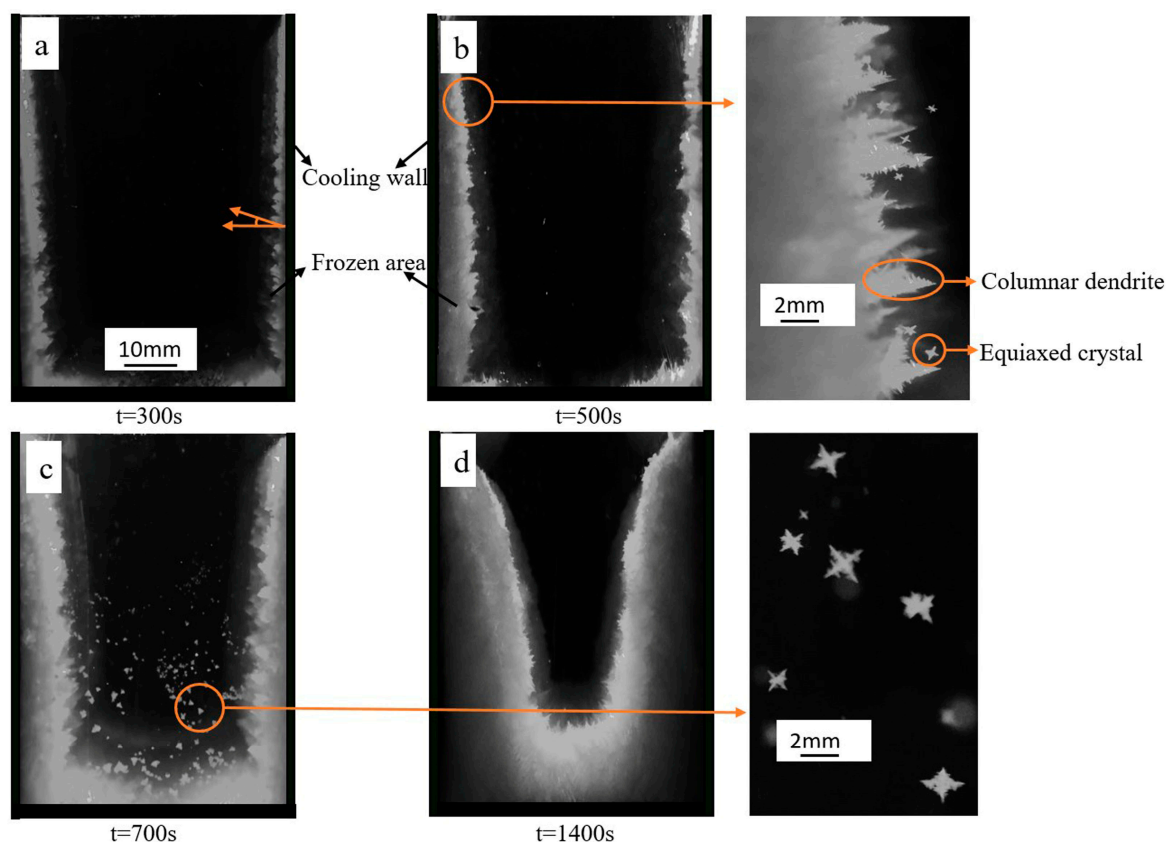


Figure 3. Solidification morphology in the melt at selected times.

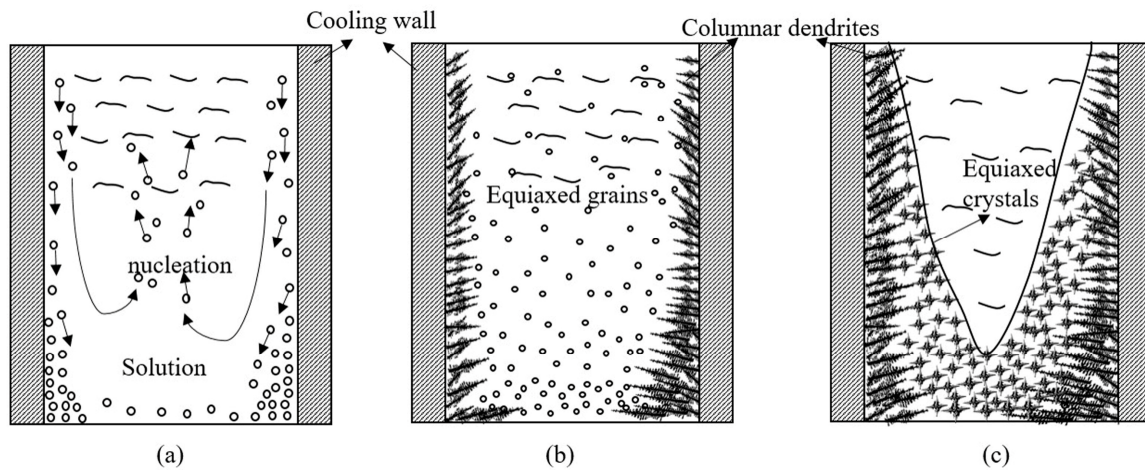


Figure 4. The schematic diagram of the development of various microscopic structural zones in a cast mold (a) initial stage; (b) mediate stage; (c) final stage.

To investigate the motion of the free crystals, which further promote the CET, an isolated NH_4Cl crystal was traced. With the progress of solidification, natural convection within the section around a plume was induced by the thermo-solutal buoyancy. Thus, an upward flow within the interdendritic liquid is formed which spews many dendrite fragments into the bulk liquid [19]. Some of the fragments dissolved when they met the melt at a temperature above the liquidus. The other fragments survived as the sources of the equiaxed grains when they reached the liquid at a temperature below the liquidus. The equiaxed grains rejected from the sidewalls began to grow until they reached a size when gravity dominated over other forces, then they started to sink. Some of the equiaxed crystals settled to the bottom of the cavity. During the settling, a coalescence could have occurred between the two small crystals after they collided, which could have promoted the settling. The coalescence between two crystals during sinking is shown in Figure 5. These settled crystals formed a sediment bed. There also were some equiaxed crystals that followed the convective flow and interacted with columnar dendrites front where they were captured. As shown in Figure 6, the position variation of the traced crystal has been marked with a circle. When the captured crystals as well as the sediment bed increased to the height corresponding to the location, the growth of the columnar dendrite front was blocked there [20]. Afterwards, the CET occurred.

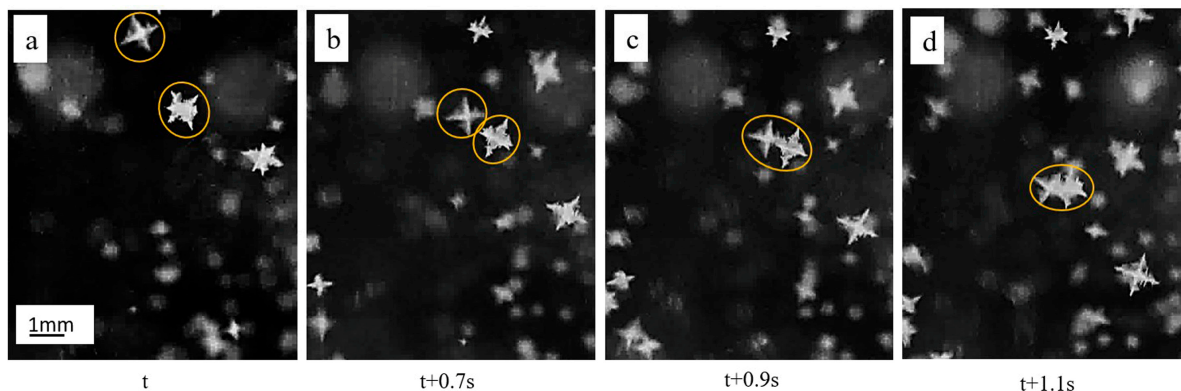


Figure 5. The coalescence between two crystals during sinking.

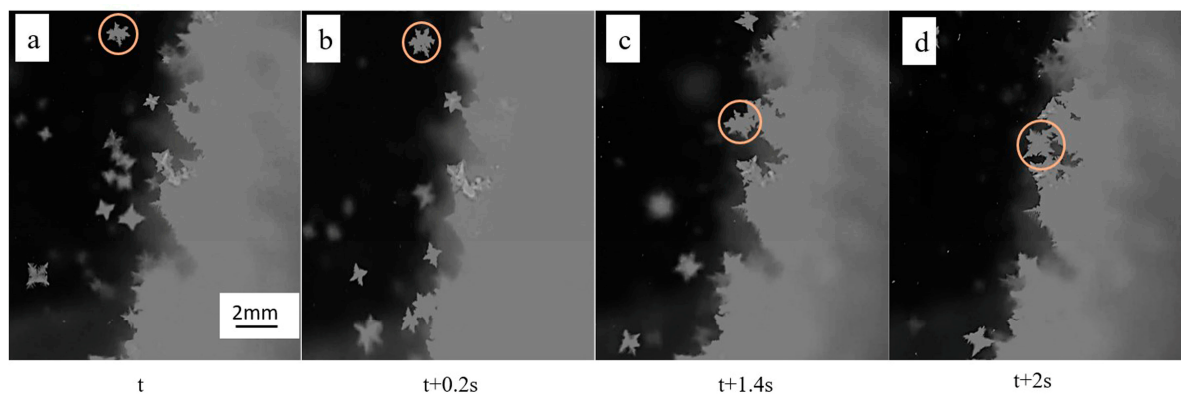


Figure 6. Illustration of the process of a downward moving equiaxed crystal captured by the solidified side wall.

3.2. Effect of Cooler on the Solidification Morphology

After the solution was poured into the cavity, the cooler was equipped to the top surface center and immersed into the solution. The solidification morphology in the cavity at selected moments with a cooler is shown in Figure 7. After the immersion of the cooler, the degree of supercooling was sufficient in the center to generate the nucleation. Thus, a large amount of nucleation generated around the cooler and developed into equiaxed grains. The equiaxed grains attached to the cooler surface resulted in the increase of cooler thickness. Afterwards, the attached grains grew to equiaxed crystals and sank into the bulk liquid. After 200 s, the cooler began to melt. It can be observed that the dendrites that split off from the cooler remarkably increased the amount of free equiaxed crystals. As the movement of free crystals is driven by the density difference between solid and liquid, the natural convection in the cooler adding zone was enhanced. Thus, the crystal rain introduced by the cooler expanded from the central zone to the whole domain. The overall freezing method simultaneously was altered both internally and externally. The acceleration of the sediment bed growth also promoted the occurrence of CET. Moreover, the size of the equiaxed crystals introduced by the cooler was smaller than those grown from the free crystal rain. This is because with the continuous changes in temperature and solute concentration, the convection is enhanced, and the moving crystal grains in the solution will repeatedly undergo local dissolution and growth, which will cause the refinement of crystals [21]. The schematic diagram of the mechanism of the grain refinement is depicted in Figure 8. In addition, it can be found that the freezing process accelerates with an increase of heat loss rate. The amount of introduced free crystals increases and the size of the crystals decreases with the increase of the cooler thickness. This is because when a thicker cooler is employed, more surrounding solution could be cooled to promote the formation of nucleation. At the same time, more dendrites split off from the cooler are potential nuclei for new grains, promoting the widening of the equiaxed zone.

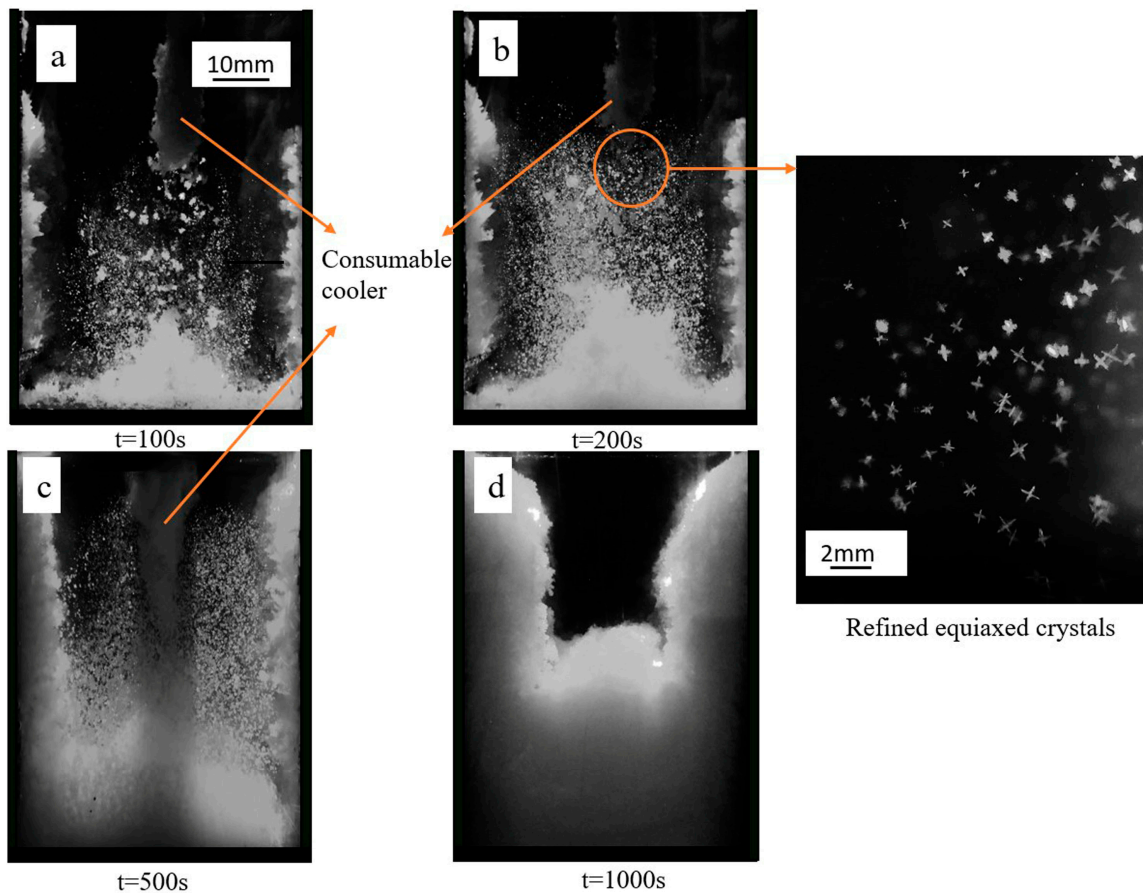


Figure 7. Solidification evolution in the cavity with a consumable cooler introduced inside.

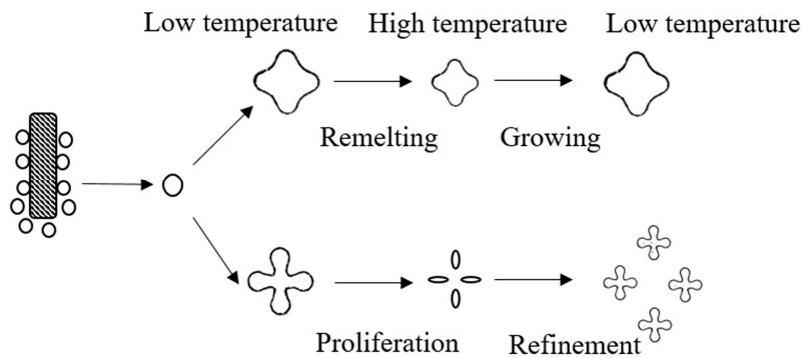


Figure 8. Schematic diagram of the mechanism of the grain refinement.

3.3. Effect of Adding Cooler on the Temperature Profile

The measured temperature variation at different horizontal positions, with and without a cooler, was plotted in Figure 9. The solution in all cases were heated to 85 °C. Zero point of time is the moment when sidewall chilling started. In the reference experiment (without cooler), a relatively rapid drop in temperature at position T3 occurred in the initial stage because of the large temperature gradient imposed by the cooling wall. During this period, the temperature at the central position of the cavity (T1 and T2) decreased gradually. After about 200 s, the decrease of the three temperatures followed a similar tendency. Also, the temperature distribution between the three measuring points exhibited horizontal thermal stratification as the solution was cooled from the sidewalls to the center.

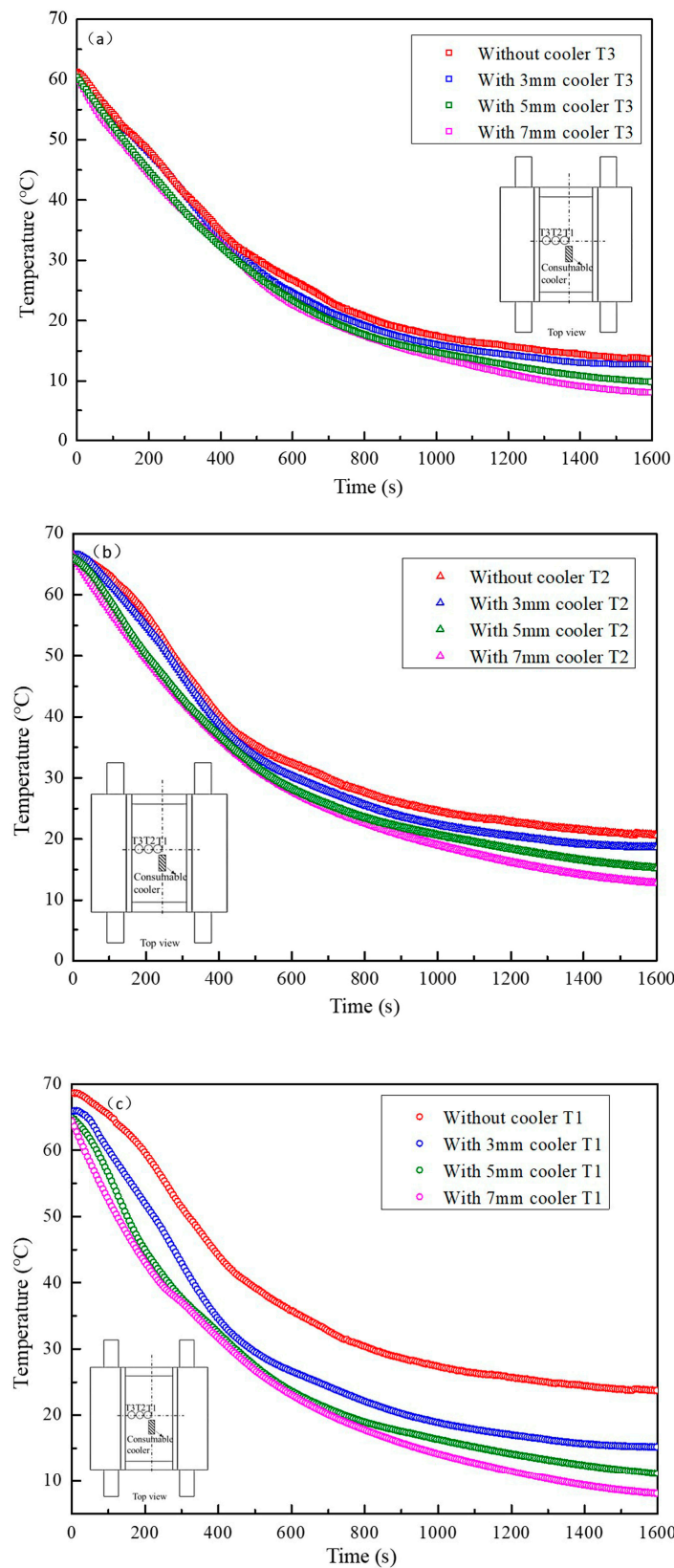


Figure 9. The measured temperature variation at different horizontal positions (a) position T3; (b) position T2; (c) position T1.

In the experiments with a cooler, in the initial stage, the temperature at position T1 dropped quickly due to the solid cooler. At the same time, the temperature at position T2 decreased because of

the cooling diffusion. The region near the cavity center was cooler than other locations. This situation is different from the reference case of cooling from external to internal. Under the combined cooling effect of the internal cold source and external cooling, the overall heat dissipation rate of the cavity was significantly accelerated. As a result, the decrease of the temperatures at positions T2 and T3 was accelerated. In addition, the cooling effect of the cooler increases with the cooler thickness. A thicker cooler led a lower temperature. It can be seen that for T2, it takes 140 s less for the 7 mm cooler to drop to 25 degrees compared with the 3 mm cooler. The final temperature in the cavity center for the 7 mm cooler is also seven degrees lower than that for the 3 mm one. Studies show that the larger cooling rate will promote the formation of finer grains, thus the amount of refined equiaxed grains in the mold increases with the increase of cooler thickness [22,23].

The temperature gradients among the three points with and without the cooler are plotted in Figure 10. The temperature gradient is defined as the temperature difference divided by the distance between the two thermocouples, as T1-T2 and T2-T3 ($^{\circ}\text{C}/\text{cm}$). In all cases, variation of the temperature gradients can be divided into three periods: first increasing, then decreasing and finally increasing to a stabilized value. In the initial stage, the temperature gradient increased firstly because the initial period is dominated by cooling conduction. Later, with the progress of solidification in the solid-liquid interface and under the effect of latent heat release and the double-diffusive convection, the temperature gradient drops. Finally, the temperature gradient magnitude returns to a stabilized value after the solid-liquid interface has passed through that location. With a cooler, the temperature gradient between T1 and T2 turned negative, but the absolute magnitude of the difference increased. The temperature gradient between T2 and T3 decreased as temperature at T2 dropped faster under the effect of enhanced cooling. It is observed that while the wall temperature reached a lower limit, the temperature gradient between T2 and T3 decreased gradually in the later stage of solidification. It is observed in the reference experiment that the CET occurs after the solid-liquid interface moved over T2, where columnar and equiaxed crystals co-exist. The CET occurs in the presence of a relatively low temperature gradient (about 2.8°C). With a cooler, the CET occurs after the solid-liquid interface developed over the T3 (between T3 and T2). The achieved temperature gradient (as high as 6.2°C) during the CET period is much larger than that of the reference experiment. This indicates that while under the solution at a high temperature gradient, when a large number of nucleation is introduced into the bulk solution, the triggered equiaxed crystal rain can also promote the CET significantly. With the increase of cooler thickness, the temperature gradient increased in the early stages, which depresses the growing rate of crystal [24,25]. As such, a thicker cooler will promote the refinement of the crystals.

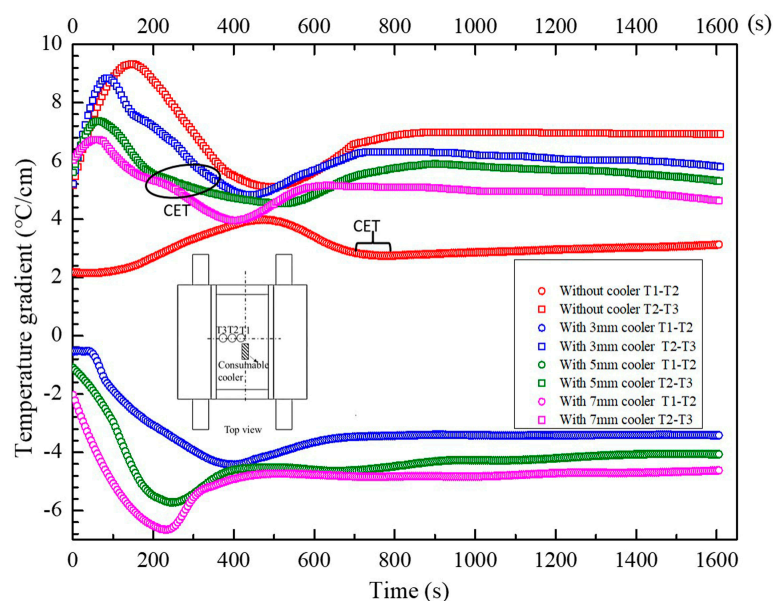


Figure 10. The temperature gradients between the three points with and without adding cooler.

4. Conclusions

Experiments were conducted to study the solidification of NH_4Cl -70% H_2O solution in a cavity with two cooled side walls. The effect of adding a consumable cooler with different thickness into the cavity was studied. The morphology variation of the crystals and the temperature distribution during the process were recorded. The main conclusions are as follows:

- (1) The solidification process can be divided into three periods: pure columnar dendrites growth, equiaxed crystal rain occurrence, equiaxed crystal block the columnar growth to a steady state.
- (2) Introduction of the consumable cooler can significantly reduce the temperature of the central zone of mold. Melting of the consumable cooler can supply large quantity of equiaxed grains and refine the crystal size. The introduced equiaxed crystals can block the growth of columnar dendrites, thereby promoting the CET.
- (3) In the reference experiment without a cooler, CET occurs when the temperature gradient decreased to $2.8\text{ }^\circ\text{C}$. In the experiment with a consumable cooler included, the CET occurs even if the temperature gradient is as high as $6.2\text{ }^\circ\text{C}$.
- (4) The consumable cooler with a larger thickness can introduce more equiaxed crystals with smaller sizes. Thus, the solidification rate and the compactness of the solidified structure increased.

Author Contributions: R.N. and B.L. designed the experiments; R.N., Z.L. and L.B. analyzed the results; X.L., X.Y. and F.T. assisted in data analysis and revised manuscript.

Funding: The authors' gratitude goes to National Natural Science Foundation of China (51574068 and 51604070) and Young Elite Scientists Sponsorship Program by China Association for Science and Technology (CAST).

Conflicts of Interest: The authors declare no conflict of interest.

References

1. Xu, Z.; Wang, X.; Jiang, M. Investigation on improvement of center porosity with heavy reduction in continuously cast thick slabs. *Steel Res. Int.* **2017**, *88*, 1600061. [[CrossRef](#)]
2. Liu, Z.; Liu, X.; Chunhui, H.U.; Mao, W. Research on fractal characteristics of primary phase morphology in semi-solid a356 alloy. *Acta Metall. Sin.* **2009**, *535–537*, 936–940. [[CrossRef](#)]
3. Xu, Y.; Wang, E.G.; Li, Z.; Deng, A.Y. Effects of vertical electromagnetic stirring on grain refinement and macrosegregation control of bearing steel billet in continuous casting. *J. Iron Steel Res. Int.* **2017**, *24*, 483–489. [[CrossRef](#)]
4. Xu, Z.; Yan, J.; Chen, W.; Yang, S. Effect of ultrasonic vibration on the grain refinement and sic particle distribution in Zn-based composite filler metal. *Mater. Lett.* **2008**, *62*, 2615–2618. [[CrossRef](#)]
5. Ludwig, A.; Stefan-Kharicha, M.; Kharicha, A.; Wu, M. Massive formation of equiaxed crystals by avalanches of mushy zone segments. *Metall. Mater. Trans. A* **2017**, *48*, 2927–2931. [[CrossRef](#)]
6. Rauter, D.I.W.; Reiter, J.; Srienc, K.; Brandl, W.; Erker, M.; Huemer, K. Soft reduction at a round bloom caster: Implementation and results. *BHM Berg-und Hüttenmännische Monatshefte* **2014**, *159*, 454–460. [[CrossRef](#)]
7. Golenkov, M.A. Improvement of internal quality of continuously cast slabs by introducing consumable vibrating macrocoolers in a mold. *Russ. Metall.* **2014**, *12*, 961–965. [[CrossRef](#)]
8. Nosochenko, O.V.; Isaev, O.B.; Lepikhov, L.S.; Degtyarev, P.A.; Kharchevnikov, V.P.; Mel'Nik, N.P. Reducing axial segregation in a continuous-cast semifinished product by micro-alloying. *Metallurgist* **2003**, *47*, 244–247. [[CrossRef](#)]
9. Isaev, O.B. Effectiveness of using large cooling elements to alleviate axial segregation in continuous-cast ingots. *Metallurgist* **2005**, *49*, 324–331. [[CrossRef](#)]
10. Habu, Y.; Itoyama, S.; Emi, T.; Sorimachi, K.; Kojima, H. Improvement cast structure and centerline segregation of continuously cast slabs by adding steel strip into mold. *Tetsu-to-Hagane* **1981**, *67*, 92–101. [[CrossRef](#)]
11. Jackson, K.A.; Hunt, J.D. Transparent compounds that freeze like metals. *Acta Metall.* **1965**, *13*, 1212–1215. [[CrossRef](#)]

12. Christenson, M.S.; Incropera, F.P. Solidification of an aqueous ammonium chloride solution in a rectangular cavity. *Int. J. Heat Mass Transfer* **1989**, *32*, 47–68. [[CrossRef](#)]
13. Tatsuo, N.; Masaki, F.; Namiko, H.; Hisashi, M. Temperature visualizations by use of liquid crystals of unsteady natural convection during supercooling and freezing of water in an enclosure with lateral cooling. *Int. J. Heat Mass Transfer* **1991**, *34*, 2663–2668. [[CrossRef](#)]
14. Beckermann, C.; Wang, C.Y. Equiaxed dendritic solidification of a $\text{NH}_4\text{Cl-H}_2\text{O}$ solution with convection 3 comparisons with $\text{NH}_4\text{Cl-H}_2\text{O}$ experiments. *Metall. Mater. Trans. A* **1998**, *27*, 2784–2795. [[CrossRef](#)]
15. Shigeo, A.; Takahiko, S.; Iwwo, M. Theoretical analysis and model study of the formation of A-type segregation in ingot. *ISIJ Int.* **1977**, *63*, 1512–1519.
16. Kharicha, A.; Stefan-Kharicha, M.; Ludwig, A.; Wu, M. Simultaneous observation of melt flow and motion of equiaxed crystals during solidification using a dual phase particle image velocimetry technique. part ii: Relative velocities. *Metall. Mater. Trans. A* **2013**, *44*, 661–668. [[CrossRef](#)]
17. Zhong, H.; Zhang, Y.; Chen, X.; Wu, C.; Wei, Z.; Zhai, Q. In situ observation of crystal rain and its effect on columnar to equiaxed transition. *Metals* **2016**, *6*, 271. [[CrossRef](#)]
18. Hellawell, A.; Liu, S.; Lu, S.Z. Dendrite fragmentation and the effects of fluid flow in castings. *JOM* **1997**, *49*, 18–20. [[CrossRef](#)]
19. Hellawell, A.; Sarazin, J.R.; Steube, R.S. Channel convection in partly solidified systems. *Philos. Trans. Phys. Sci. Eng.* **1993**, *345*, 507–544.
20. Jie, W.; Zhou, X. Experimental study on the columnar to equiaxed transformation process. *J. Northwest. Polytech. Univ.* **1988**, *6*, 35–46.
21. Glicksmann, M.E. *The solidification of metals*; The Iron and Steel Institute: London, UK, 1967; p. 43.
22. Huang, W.D.; Wang, W.L.; Lin, X.; Wang, M. In situ observation of SSM microstructure formation during cooling slope casting of an $\text{NH}_4\text{Cl-H}_2\text{O}$ alloy with vibrating the slope. *Solid State Phenom.* **2006**, *116–117*, 193–196. [[CrossRef](#)]
23. Trivedi, R.; Kurz, W. Dendritic growth. *Int. Met. Rev.* **1994**, *39*, 49–74. [[CrossRef](#)]
24. Lu, C.W.; Chen, J.C.; Hu, L.J. A numerical investigation of the thermal distribution effects in a heat-exchanger-method crystal growth system. *Model. Simul. Mater. Sci. Eng.* **2002**, *10*, 147. [[CrossRef](#)]
25. Shi, Y.; Qingyan, X.U.; Gong, M. Simulation of $\text{NH}_4\text{Cl-H}_2\text{O}$ dendritic growth in directional solidification. *Acta Metall. Sin.* **2011**, *47*, 620–627.



© 2019 by the authors. Licensee MDPI, Basel, Switzerland. This article is an open access article distributed under the terms and conditions of the Creative Commons Attribution (CC BY) license (<http://creativecommons.org/licenses/by/4.0/>).